AIP Applied Physics Letters

An electrical injection metallic cavity nanolaser with azimuthal polarization

Kang Ding, Leijun Yin, Martin T. Hill, Zhicheng Liu, Peter J. van Veldhoven et al.

Citation: Appl. Phys. Lett. **102**, 041110 (2013); doi: 10.1063/1.4775803
View online: http://dx.doi.org/10.1063/1.4775803
View Table of Contents: http://apl.aip.org/resource/1/APPLAB/v102/i4
Published by the American Institute of Physics.

APPLIED PHYSICS LETTERS **102**, 041110 (2013)

An electrical injection metallic cavity nanolaser with azimuthal polarization

Kang Ding,[1] Leijun Yin,[1] Martin T. Hill,[2] Zhicheng Liu,[1] Peter J. van Veldhoven,[2] and C. Z. Ning[1,a)]
[1]*School of Electrical, Computer, and Energy Engineering, Arizona State University, Tempe, Arizona 85287, USA*
[2]*COBRA Research Institute, Technische Universiteit Eindhoven, 5600 MB Eindhoven, The Netherlands*

(Received 12 October 2012; accepted 19 December 2012; published online 29 January 2013)

We demonstrated for the first time an azimuthally polarized laser source from an electrically driven metallic cavity nanolaser with a physical cavity volume of 0.146 λ^3 ($\lambda = 1416$ nm). Single TE_{01} mode lasing at 78 K was achieved by taking the advantages of the large free spectral range in such nanoscale lasers and the azimuthal polarization of lasing emission was verified experimentally. Mode shift controlled by device cavity radius was observed over a large wavelength range from 1.37 μm to 1.53 μm. Such metallic cavity nanolaser provides a compact electrically driven laser source for azimuthally polarized beam. © *2013 American Institute of Physics*. [http://dx.doi.org/10.1063/1.4775803]

The emerging of metallic cavity nanolasers[1–3] and spasers[4–6] has greatly impacted the development of semiconductor lasers as a new strategy for the miniaturization of lasers.[7] As a byproduct of such miniaturization, purposeful selection of single mode of specific properties becomes possible, especially the mode with a specific polarization. Among various realizations of nanolasers,[8–16] devices with circular geometry exhibit interesting polarization properties. Radially polarized lasing emission was observed in a metallic coaxial nanolaser.[13] Yu *et al.*[16] reported lasing emission with azimuthal polarization from nanopatch lasers. As a subset of cylindrical vector beams, azimuthally polarized beam has special applications such as particle trapping[17] and high resolution imaging.[18] Numerous approaches have been developed to generate azimuthally polarized light beams, including inserting optical components into YAG laser cavities[19,20] to select the lasing mode. Optical fibers[21] and dielectric gratings[22] were utilized to convert light beam to azimuthal polarization as well. However, these methods are generally cumbersome. Incorporating surface grating has been proven as an effective approach to realize polarization control and stabilization in vertical cavity surface emitting lasers (VCSELs).[23] Compact light sources based on this approach for radially polarized beam have been demonstrated.[24] The two aforementioned examples of metallic cavity nanolasers with radial[13] and azimuthal[16] polarizations are both under optical pumping. To our best knowledge, there has not been any report on the realization of a compact nanoscale electrically driven laser source with azimuthal polarization.

As we will demonstrate in this paper, our metallic cavity nanolaser exhibits single TE_{01} mode lasing with azimuthal polarization. More importantly, this electrically driven laser greatly simplifies its implementation in practical applications. The device structure is shown in Fig. 1. An InP/InGaAs/InP layer stack grown by metal organic chemical vapor deposition (MOCVD) is etched into circular pillars and then we deposit SiN layer via plasma enhanced chemical vapor deposition (PECVD) for insulating purpose and also as a buffer layer to push away optical field from lossy metal to improve cavity quality factor (Q).[25] Finally, the whole structure is encapsulated in silver to form a metallic cavity. Electrical injection is enabled through top and bottom contacts. Detailed fabrication process is described in our previous publication.[26] In this device, the vertical optical confinement is not achieved through metal mirror or distributed Bragger reflector[14] (DBR), but by trapping optical mode in the InGaAs segment with a higher refractive index. Through finite difference time domain (FDTD) simulation, we calculated the resonance wavelengths of the three lowest order modes HE_{11}, TM_{01}, and TE_{01} in the metallic nanocavity as a function of semiconductor pillar radius (see Fig. 2(a)). The free spectral ranges of these three modes are very large such that only one mode will fall within the gain bandwidth of InGaAs material for a given radius. Thus, operation of a single mode can be easily achieved. As shown in Fig. 2(a), mode resonance wavelength shifts almost linearly with radius through the entire InGaAs gain bandwidth. All these features allow easily controllable realization of a single specific mode with the associated polarization properties by adjusting device radius during the lithography step.

Among those three lowest modes, the TE_{01} (see Fig. 2(b)) is particularly interesting. The electric field of TE_{01} mode is dominated by the azimuthal component which is parallel to the surface of metal and has least interaction with metal or in other words less metal loss. Therefore, relatively high cavity quality factor (Q) can be achieved for TE_{01} mode in a deep sub-wavelength metallic nanocavity. From our simulation, the Q value of TE_{01} mode in a cavity with semiconductor pillar radius of 190 nm and optimized SiN thickness of 120 nm (total cavity physical volume 0.125 λ^3, $\lambda = 1543$ nm) is 363, corresponding to a threshold material gain of 959 cm^{-1} which is achievable at room temperature under electrical injection. The output emission of TE_{01} mode in free space will preserve such azimuthal polarization. Fig. 2(c) shows the simulated azimuthal electric field of TE_{01} mode outside the cavity in the substrate. The azimuthal electric field is the dominant component and shows a "donut" shape.

a)Author to whom correspondence should be addressed. Electronic mail: cning@asu.edu.

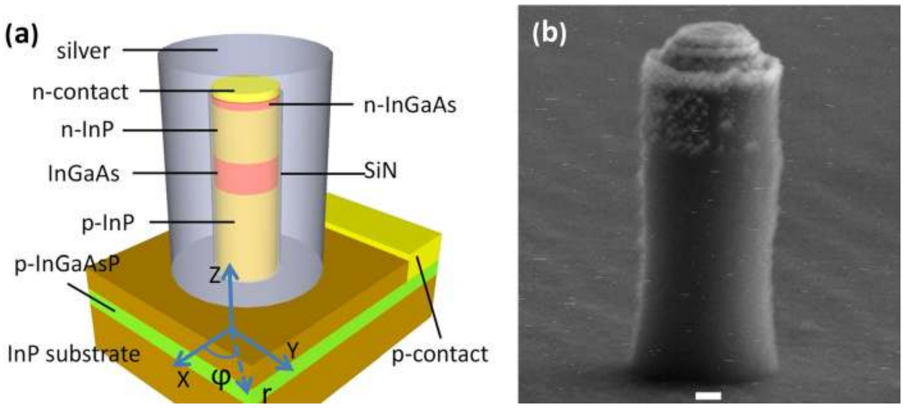

FIG. 1. (a) Structure of a metallic cavity nanolaser with circular cross section. (b) Scanning electron microscope image of an InP/InGaAs/InP nano-pillar coated with SiN layer on its sidewall. We etched away the SiN on top of the pillar and deposited Ti/Pt/Au thus forming the top n contact. Scale bar is 100 nm.

Therefore, the laser beam from such devices supporting TE_{01} mode will be azimuthally polarized.

We fabricated a series of devices with semiconductor pillar radius from 165 nm to 250 nm and SiN layer thickness at 120 nm. Measurements with DC current injection were performed at 78 K. Light output from a device was collected by a 50× objective with 0.5 numerical aperture. Passing through a beam splitter, half of the light was detected by a spectrometer equipped with a liquid nitrogen cooled InGaAs array detector and the other half was directed to an InGaAs near infrared (NIR) camera for imaging. Continuous wave (CW) lasing was achieved at 78 K. Fig. 3(a) shows lasing characteristics from a device with a semiconductor pillar radius of 175 nm and a total cavity volume of 0.146 λ^3 ($\lambda = 1416$ nm), including SiN layer. The L-I curve shows a threshold current around 80 μA. The saturation of the spontaneous emission confirms the lasing behavior. We also observed a linear resonance wavelength shift over a large wavelength range from 1.37 μm to 1.53 μm on devices with different radii (see Fig. 3(b)). A shifting slope defined as $\Delta\lambda/\Delta$d (λ: resonance wavelength, d: semiconductor pillar diameter) from the experimental result is 2.7, (shown in Fig. 2(a)) which matches the value of 3.1 for TE_{01} mode from simulation quite well. To confirm the azimuthal polarization of the lasing beam, we took the images of the laser output after inserting a linear polarizer between the objective and camera.[27] The azimuthal polarization is characterized by the dark line splitting the images along the polarizer direction (see Fig. 3(c)). Hence, we demonstrate a compact nanoscale electrically driven laser source for azimuthally polarized beam based on a metallic cavity nanolaser supporting TE_{01} mode.

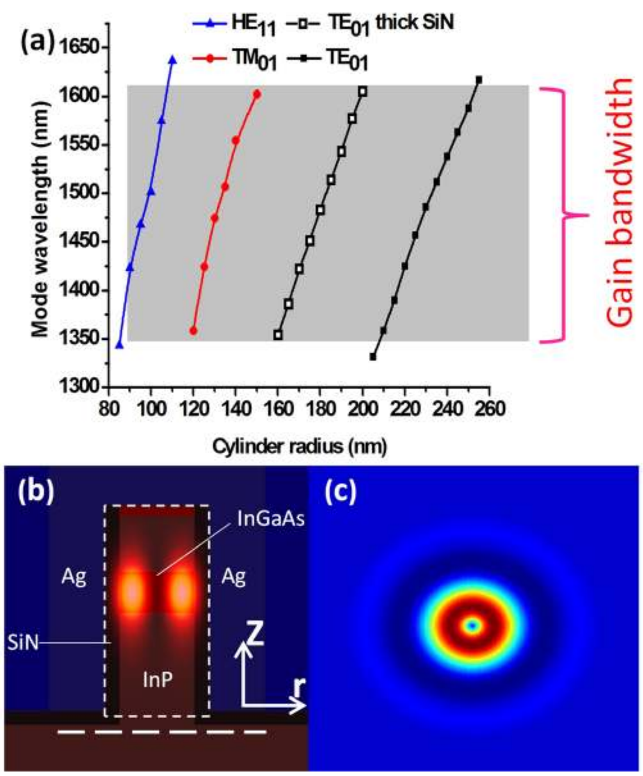

FIG. 2. (a) Resonance wavelengths of HE_{11}, TM_{01}, and TE_{01} modes in a metallic cavity nanolaser as a function of semiconductor pillar radius. Thickness of SiN layer is 30 nm for all the curves except the one with unfilled squares, for which SiN thickness is 120 nm. Shaded gray region indicates roughly the gain bandwidth of InGaAs material. (b) $|E|^2$ field of TE_{01} mode in Z-r plane. Cavity boundary is marked by white dashed rectangle. (c) Azimuthal component of the electric field of TE_{01} mode beneath the cavity bottom aperture at the vertical location in r-φ plane, indicated by the white long dashed line in (b).

Compared to other compact light sources for cylindrical vector beams, such as the surface grating VCSELs reported by Cai *et al.*,[24] our device is not only smaller but also offers a reduction in fabrication complexity. First, vertical confinement in our nanolaser is achieved through trapping optical mode in high refractive index gain material instead of reflection by DBR, thus eliminating the need for complex DBR layer stack growth. Second, desired single TE_{01} mode lasing can be ensured easily by controlling the radius of semiconductor pillar in lithography step, while design and fabrication of surface grating for VCSELs is generally more sophisticated. On the other hand, the linewidth of our nanolaser is about 2 nm, much broader than VCSELs.[14,28] Such broad linewidth is often seen in recently reported deep subwavelength metallic cavity nanolasers[13,16,26] and can be attributed to several reasons. First, due to the use of lossy metal, small physical volume and lack of high reflection DBR layers, the Q factor of metallic cavity nanolaser currently is generally lower than conventional semiconductor lasers including VCSELs. Therefore, the operation of metallic cavity nanolaser is often limited to high threshold and low output power, which eventually leads to broad linewidth.[3,26] Second, the spontaneous emission factor β, the portion of spontaneous emission coupled into the lasing mode, increases in such small cavities and will broaden the linewidth as well.[29] Detailed discussion on linewidth of such metallic cavity nanolasers is beyond the scope of this paper.

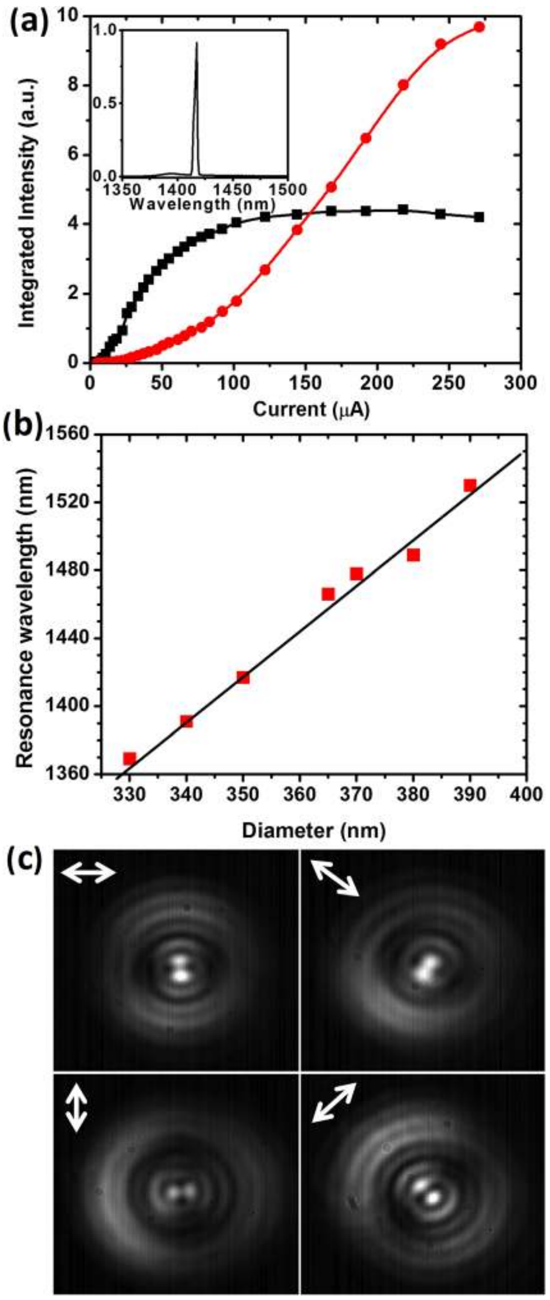

FIG. 3. (a) CW lasing characteristics from a device with total cavity volume of 0.146 λ^3 ($\lambda = 1416$ nm). L-I curve shows a threshold current at 80 μA. Inset is the lasing spectrum at 196 μA. (b) Linear dependence of resonance wavelength on diameter from 1.37 μm to 1.53 μm, where the slope is 2.7. (c) Laser output images taken by a NIR camera behind a linear polarizer in four different orientations, as indicated by the white arrow. The dark line splitting the image along the polarizer direction confirms the azimuthal polarization of the laser output.

A major concern or drawback of this metallic cavity nanolaser is the relatively large divergence angle of its output beam, given the fact that the lasing emission inside the cavity has to pass through a sub-wavelength aperture to escape to the free space. For many applications, low divergence beam with better directivity is preferred. Hill and Marell[30] proposed a solution to improve the output beam quality of nanolasers supporting HE_{11} mode by including a horn antenna waveguide structure in the bottom cladding part of the cavity as shown in Fig. 4(a). This approach also applies to this TE_{01} mode nanolasers. Simulation result in Fig. 4(b) shows that the

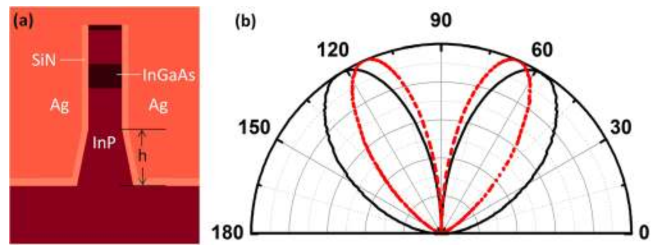

FIG. 4. (a) Schematic of metallic cavity nanolaser with horn-shaped antenna waveguide. (b) Far field radiation pattern (|E|) of the nanolaser. Red dashed curve corresponds to device with a horn antenna, showing both narrower far-field lobes and smaller angle separation of two lobes than straight sidewall device (black solid line). The angle in this plot is with respect to the cavity aperture plane and 90° is the direction normal to the aperture plane.

angle separation between the maxima of the two lobes of TE_{01} mode reduces from 64° to 46° after including a horn structure with the angle width of each reduced from 31° to 22°. The improved beam divergence angle (full angle at half maximum intensity) is 74°, which is about 3–4 times the value of VCSELs with a much larger aperture diameter on the order of microns.[31] Though this divergence is still too large for direct implementation in certain practical on-chip applications and on-chip microlens will be required for collimation or focusing,[32] we think improved beam quality may help to relieve requirements on such micro-optics needed. The height of the tapered region in this simulation is h = 700 nm and its sidewall tilting angle is 20°. Since the sidewall angle of InP pillar can be controlled in the CH_4/H_2 inductively coupled plasma etching process by adjusting etching parameters,[33] this horn antenna waveguide structure is indeed achievable in our fabrication.

In conclusion, we demonstrated CW lasing from a metallic cavity nanolaser with a total cavity volume of 0.146 λ^3 ($\lambda = 1416$ nm) under electrical injection. The azimuthal polarization of the output beam is verified. To our knowledge, this is the first report of a nanoscale laser source with electrical injection for azimuthally polarized beam. Some features of this device, such as single mode operation and tunable lasing wavelength over a large range, could be desirable for certain applications. Potential improvement of beam quality using a horn antenna structure is also demonstrated through a simulation. Currently, the CW operation temperature of our device is limited to 78 K, far below the room temperature as predicted in our simulation. We believe that the reason can mainly be attributed to the device degradation due to poor heat dissipation and surface recombination related to the thick SiN layer (120 nm) used. Through optimizing device design and improving fabrication, it is possible to reduce the lasing threshold and alleviate the thermal issue, so that improved device performances including narrower linewidth and room temperature operation are expected.

This work was supported by the Defense Advanced Research Project Agency (DARPA) program Nanoscale Architectures of Coherent Hyper-Optical Sources (NACHOS, W911-NF07-1-0314) and by the Air Force Office of Scientific Research (FA9550-10-1-0444, Gernot Pomrenke). We acknowledge Advanced Computing Center at Arizona State University for the support in numerical simulation.

[1]M. T. Hill, Y. S. Oei, B. Smalbrugge, Y. Zhu, T. de Vries, P. J. van Veldhoven, F. W. M. van Otten, T. J. Eijkemans, J. P. Turkiewicz, H. de Waardt, E. J. Geluk, S. Kwon, Y. Lee, R. Nötzel, and M. K. Smit, Nat. Photonics **1**, 589 (2007).
[2]A. V. Maslov and C. Z. Ning, Proc. SPIE **6468**, 64680I (2007).
[3]K. Ding and C. Z. Ning, Light: Sci. Appl. **1**, e20 (2012).
[4]D. J. Bergman and M. I. Stockman, Phys. Rev. Lett. **90**, 027402 (2003).
[5]M. A. Noginov, G. Zhu, A. M. Belgrave, R. Bakker, V. M. Shalaev, E. E. Narimanov, S. Stout, E. Herz, T. Suteewong, and U. Wiesner, Nature **460**, 1110 (2009).
[6]N. I. Zheludev, S. L. Prosvirnin, N. Papasimakis, and V. A. Fedotov, Nat. Photonics **2**, 351 (2008).
[7]C. Z. Ning, Phys. Status Solidi B **247**, 774 (2010).
[8]M. T. Hill, M. Marell, E. S. P. Leong, B. Smalbrugge, Y. Zhu, M. Sun, P. J. van Veldhoven, E. J. Geluk, F. Karouta, Y. S. Oei, R. Nötzel, C. Z. Ning, and M. K. Smit, Opt. Express **17**, 11107 (2009).
[9]R. F. Oulton, V. J. Sorger, T. Zentgraf, R. M. Ma, C. Gladden, L. Dai, G. Bartal, and X. Zhang, Nature **461**, 629 (2009).
[10]R. Ma, R. F. Oulton, V. J. Sorger, G. Bartal, and X. Zhang, Nature Mater. **10**, 110 (2011).
[11]R. Perahia, T. P. Mayer, A. H. Safavi-Naeini, and O. Painter, Appl. Phys. Lett. **95**, 201114 (2009).
[12]M. J. H. Marell, B. Smalbrugge, E. J. Geluk, P. J. van Veldhoven, B. Barcones, B. Koopmans, R. Nötzel, M. K. Smit, and M. T. Hill, Opt. Express **19**, 15109 (2011).
[13]M. Khajavikhan, A. Simic, M. Katz, J. H. Lee, B. Slutsky, A. Mizrahi, V. Lomakin, and Y. Fainman, Nature **482**, 204 (2012).
[14]C. Y. Lu, S. W. Chang, S. L. Chuang, T. D. Germann, and D. Bimberg, Appl. Phys. Lett. **96**, 251101 (2010).
[15]M. P. Nezhad, A. Simic, O. Bondarenko, B. Slutsky, A. Mizrahi, L. Feng, V. Lomakin, and Y. Fainman, Nat. Photonics **4**, 395 (2010).
[16]K. Yu, A. Lakhani and M. C. Wu, Opt. Express **18**, 8790 (2010).
[17]F. Peng, B. Yao, S. Yan, W. Zhao, and M. Lei, J. Opt. Soc. Am. B **26**, 2242 (2009).
[18]Q. Zhan, Adv. Opt. Photon **1**, 1 (2009); J. R. Zurita-Sánchez and L. Novotny, J. Opt. Soc. Am. B **19**, 2722 (2002).
[19]R. Oron, S. Blit, N. Davidson, A. A. Friesem, Z. Bomzon, and E. Hasman, Appl. Phys. Lett. **77**, 3322 (2000).
[20]M. P. Thirugnanasambandam, Y. Senatsky, and K. Ueda, Opt. Express **19**, 1905 (2011).
[21]T. Hirayama, Y. Kozawa, T. Nakamura, and S. Sato, Opt. Express **14**, 12839 (2006).
[22]Z. Bomzon, G. Biener, V. Kleiner, and E. Hasman, Opt. Lett. **27**, 285 (2002).
[23]J. M. Ostermann, P. Debernardi, C. Jalics, A. Kroner, M. Feneberg, M. C. Riedl, and R. Michalzik, Proc. SPIE **5364**, 201 (2004).
[24]L. Cai, J. Zhang, W. Bai, Q. Wang, X. Wei, and G. Song, Appl. Phys. Lett. **97**, 201101 (2010).
[25]A. Mizrahi, V. Lomakin, B. A. Slutsky, M. P. Nezhad, L. Feng, and Y. Fainman, Opt. Lett. **33**, 1261 (2008).
[26]K. Ding, Z. C. Liu, L. J. Yin, M. T. Hill, M. J. H. Marell, P. J. van Veldhoven, R. Nötzel, and C. Z. Ning, Phys. Rev. B **85**, 041301(R) (2012).
[27]We removed the beam splitter when taking the laser output images to avoid the influence of beam splitter. Also, the objective was defocused $\sim$20 μm away from the cavity bottom aperture into substrate so that the dark line in the images can be resolved.
[28]R. Shau, H. Halbritter, F. Riemenschneider, M. Ortsiefer, J. Rosskopf, G. Böhm, M. Maute, P. Meissner, and M.-C. Amann, Electron. Lett. **39**, 1728 (2003).
[29]S. Ate, C. Gies, S. M. Ulrich, J. Wiersig, S. Reitzenstein, A. Löffler, A. Forchel, F. Jahnke, and P. Michler, Phys. Rev. B **78**, 155319 (2008).
[30]M. T. Hill and M. J. H. Marell, Adv. Opt. Tech. **2011**, 314952.
[31]M. Mochizuki, T. Nishida, S. Kakinuma, and T. Kaneko, Proc. SPIE **5722**, 201 (2005).
[32]V. Bardinal, T. Camps, B. Reig, P. Debernardi, O. Soppera, D. Barat, J.-B. Doucet, and E. Daran, Proc. SPIE **8276**, 82760U (2012).
[33]H. Y. Chen, Master of Applied Science thesis, University of Toronto, 2000.